Discovery of natural adenosine monophosphate-activated protein kinase activators through virtual screening and activity verification studies

JIA HAO[1*], ZHEN YANG[2*], JIAN LI[1], LIFENG HAN[2], YI ZHANG[1] and TAO WANG[1]

[1]Tianjin State Key Laboratory of Modern Chinese Medicine, Tianjin University of Traditional Chinese Medicine; [2]Tianjin Key Laboratory of TCM Chemistry and Analysis, Institute of Traditional Chinese Medicine, Tianjin University of Traditional Chinese Medicine, Tianjin 301617, P.R. China

Received June 19, 2020; Accepted November 12, 2020

DOI: 10.3892/mmr.2021.11842

Abstract. The adenosine monophosphate-activated protein kinase (AMPK) is a promising target in drug development for various metabolic diseases. In the present study, the aim was to discover natural direct AMPK activators from natural sources, thus a virtual screening for direct AMPK activators was conducted by combining ligand-based and structure-based screening. A common-feature pharmacophore model (HipHop1) was generated with two hydrogen bond acceptor lipid features and one hydrophobic region feature. A total of 1,235 natural products were screened using the HipHop1 hypothesis and CDOCKER protocol successively. According to the docking score, seven hit compounds were selected for AMPK activation assays. Ultimately, (-)-catechin (compound 522) and licochalcone A (compound 1148) exhibited the highest AMPK activation activity. These findings may contribute to the development of AMPK activators from medicinal plants.

Introduction

The adenosine monophosphate-activated protein kinase (AMPK) is a highly conserved serine/threonine protein kinase present in almost all eukaryotic cells. It plays a key role in maintaining the balance of energy metabolism by maintaining glycogen reserves and efficient mitochondrial oxidative metabolism (1-3). Because disorders of energy balance lead to various metabolic diseases in humans, such as type-2 diabetes, inflammatory disorders, and cancer, there has been increasing interest in the development of pharmacological activators of AMPK (4-7).

According to previous structural analyses, AMPK is a heterotrimeric complex containing α, β, and γ subunits (8-11). The α subunit has two subtypes, α1 and α2, which are encoded by two separate genes and contain a catalytic serine/threonine protein kinase domain. The key phosphorylation site, Thr172, is located in this subunit. The β subunit serves as a bridge between the α and γ subunits and has two subtypes, β1 and β2, which are encoded by two separate genes. It is a regulatory unit, and the cleft between its central carbohydrate-binding module and the kinase domain in the α subunit is a critical binding site for direct activation. The γ subunit is the allosteric activation site for AMP/ADP binding. It also plays a regulatory role based on AMP/ATP and ADP/ATP ratio, and has three subtypes, γ1, γ2 and γ3, which are encoded by three different genes.

The activation of AMPK involves multiple mechanisms. Firstly, AMPK is typically activated by the phosphorylation of Thr172 in the catalytic domain of the α subunit. This process is catalyzed by multiple protein kinases such as serine threonine kinase 11 calcium/calmodulin dependent protein kinase kinase 2, and MAP3K7 (12). Secondly, allosteric activation associated with increased AMP/ATP and ADP/ATP ratios is another mechanism for AMPK activation. AMP and its mimic ADP binding to the γ subunit of AMPK not only cause allosteric effects but also protect phosphorylated Thr172 from dephosphorylation (13). Therefore, any agent that can affect the binding of AMP/ADP to the γ subunit or inhibit mitochondrial ATP production would indirectly activate the phosphorylated AMPK. Thirdly, some exogenous compounds, called direct AMPK modulators, can allosterically activate AMPK through an AMP-independent pathway. The binding site of these activators is located in the cleft between the β subunit central carbohydrate-binding module and the α subunit kinase domain (14,15).

Natural products are useful sources for drug development. Indeed, natural products coming from various medicinal

Correspondence to: Dr Yi Zhang or Dr Tao Wang, Tianjin State Key Laboratory of Modern Chinese Medicine, Tianjin University of Traditional Chinese Medicine, 10 Poyanghu Road, Jinghai, Tianjin 301617, P.R. China
E-mail: zhwwxzh@263.net
E-mail: wangtao@tjutcm.edu.cn

*Contributed equally

Key words: adenosine monophosphate-activated protein kinase, virtual screening, activity verification, activator

plants can provide abundant drug screening entities with high-molecular diversity (16). Our previous studies examined the separation and identification of natural products from traditional Chinese herbs (17-20). Based on our previous studies, a natural product library containing 1,235 compounds derived from traditional Chinese herbs with anti-metabolic effect was developed. Several of these compounds have been shown to promote AMPK activation, as curcumin, resveratrol, berberine, quercetin, and arctigenin (21-26). Moreover, whereas some of these AMPK activators can directly activate AMPK, others can also inhibit the respiratory chain and indirectly activate AMPK. Therefore, identifying the specific mechanisms of these natural activators may be beneficial for further drug development. The aim of the present study was to identify direct AMPK activators from our natural product library.

Materials and methods

Materials. Liquiritin, ononin, 5,7-dihydroxy-3',4',6-trimethoxyflavone, leonurine, (-)-catechin, luteolin, licochalcone-A were obtained from the National Institute for Food and Drug Control (Beijing, China). The HepG2 liver cancer cell line was obtained from the Cell Resource Center of Institute of Basic Medical Sciences, Chinese Academy of Medical Sciences & Peking Union Medical College. FBS was purchased from Biological Industries. Modified Eagle's medium (MEM), non-essential amino acids (NEAA), and penicillin/streptomycin were obtained from Thermo Fisher Scientific, Inc. The triglyceride (TG) assay kit (cat. no. 0220/0221/0222) was purchased from BioSino Bio-technology and Science Inc. Sodium oleate and orlistat were obtained from Sigma-Aldrich (Merck KGaA). Rabbit anti-AMPK (cat. no. 2532) and anti-β-actin (cat. no. 4970) antibodies were from Cell Signaling Technology, Inc. Rabbit anti-phosphorylated (p)-AMPK antibody (cat. no. ab133448) and HRP-conjugated secondary antibodies (cat. nos. ab6721 and ab6728) were from Abcam.

Data acquisition for protein and small molecules. The 3D structure (PDB no., 4CFE) of AMPK heterotrimeric complex (14) with three types of ligands ([staurosporine, 5-[[6-chloranyl-5-(1-methylindol-5-yl)-1H-benzimidazol-2-yl]oxy]-2-methyl-benzoic acid, and AMP) was downloaded from the Research Collaboratory for Structural Bioinformatics Protein Data Bank (http://www.rcsb.org/pdb/home). The protein structure was analyzed using Chimera 1.8.1 software (www.cgl.ucsf.edu/chimera/) and Discovery Studio 4.5 software (www.discoverystudio.net). The initial activator benzimidazole derivative 991 was extracted as a reference ligand. All of the co-ligands and water molecules were removed from the co-crystallized complex. Addition of missing hydrogen atoms and elimination of unnecessary polymers were performed using the macromolecule preparation protocol, in the Discovery Studio software. Protein structure was further analyzed using a clean protein module to correct incomplete amino acid residues and alternate conformations. Small molecules were constructed using ChemBiodraw ultra 11.0 (https://www.chemdraw.com.cn/) and employed a Chemistry at Harvard Macromolecular Mechanics (CHARMM) force field in Discovery Studio, then minimized under a Dreiding-like force field and CHARMM force field successively.

The compounds selected for virtual screening were separated and purified from traditional Chinese herbs that have anti-metabolic effects, according to our previous study. All the structures were determined by nuclear magnetic resonance spectrometry, infrared spectrum, and mass spectrometry (17-20).

Molecular docking. A molecular docking analysis was conducted using the CDOCKER module in Discovery Studio 4.5. CDOCKER is a structure-based docking method by grid calculation under the CHARMM force field (27). It is a typical semi-flexible docking protocol. The interactions between different conformations of ligands and macromolecules were collected and analyzed using a scoring algorithm. According to pre-experimental results, docking parameters were set for optimization. The binding site sphere was defined around the activated ligand 991 with a radius of 9.0 Å. Pose cluster radius was set as 0.1 Å, the number of allowed random conformations was set to 10, the number of allowed orientations was set to 10, and electrostatic interactions were included. The rest of the parameters were set as default. The top 10 conformations were saved for each ligand based on scoring function value (-CDOCKER interaction energy). To estimate whether the binding site model was sufficient for the AMPK docking system, a re-docking process was performed by evaluating the root mean squared error (RMSD) value between the initial and virtual docking conformations.

Pharmacophore model generation. The pharmacophore-based virtual screening is a ligand-based virtual screening generated from a set of active small molecules. The Common Feature Pharmacophore Generation module (HipHop) in Discovery Studio is an appropriate application for pharmacophore model generation, especially for those ligands that lack of uniform standard activity data (28). Based on published reports (Table SI; Fig. S1), 28 compounds with AMPK agonist activity were collected and divided into two sets, of which 18 compounds were in the training set, and the remaining were in the text set. The Feature Mapping function was used to identify key chemical features of the training set for predicting the considered features in the pharmacophore generation process. The principal value was set as 2, and MaxOmitFeat value was set as 0 for compounds 1-4. The principal value and MaxOmitFeat value was set as 1 for other training set compounds. Minimum Interfeature Distance was set to 2.97 Å, Minimum Features was set to 3, Feature Misses and Complete Misses was set to 0, Conformation Generation was set to 'none'. The rest of the parameters were set as default. The text set was prepared for the validation of the pharmacophore model.

Virtual screening based on pharmacophore. All the compounds that were optimized under the CHARMM force field were used as a virtual screening library in the Build 3D database module in Discovery Studio software. The screening based on pharmacophore was conducted with the Search 3D

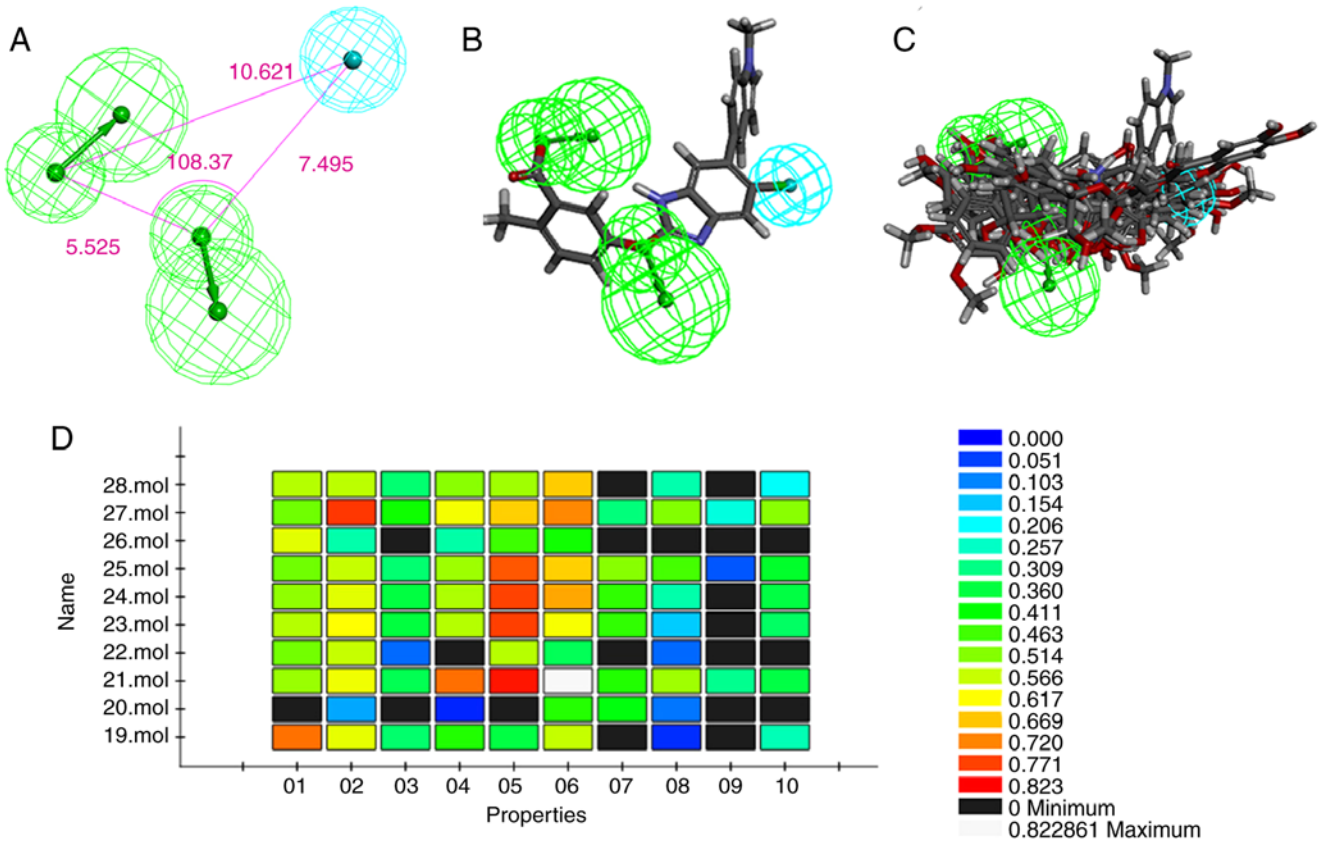

Figure 1. Pharmacophore model for AMPK activation activity. (A) HipHop1 pharmacophore hypotheses for AMPK activation activity. (B) Superposition of HipHop1 and 991. (C) Superposition of HipHop1 and training set. (D) Ligand profiler result.

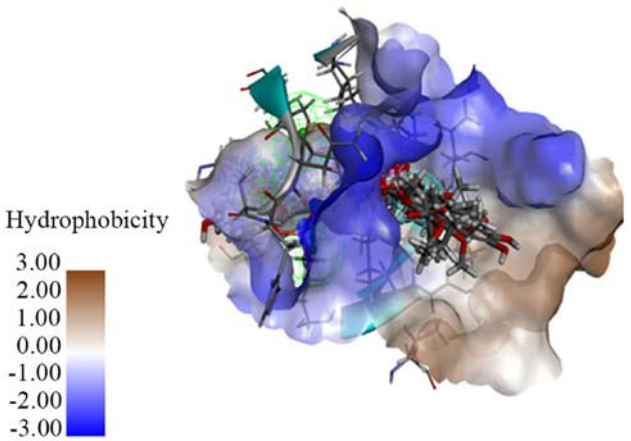

Figure 2. Pharmacophore model with hit compounds.

database function in Discovery Studio software. The search method was set as 'best'. The rest of the parameters were set as default. Hit compounds were used in subsequent molecular docking screening.

Cell culture. HepG2 cells were maintained in MEM supplemented with 1% NEAA, 10% FBS and 1% P/S, and kept in a humidified atmosphere of 5% CO_2 at 37˚C. Cells were grown to 70-80% confluence, then seeded in multi-well plates containing serum-free medium and incubated for 24 h before treatment at 37˚C with 5% CO_2.

TG accumulation inhibitory effects assay. To induce an intracellular lipid accumulation model, sodium oleate was used as previously described (29). Briefly, after seeding in 48-well plates in FBS-free medium for 24 h, HepG2 cells were exposed to 200 μM sodium oleate in the presence or absence of different compounds (3 or 30 μM), or orlistat (5 μM) as a positive control, for another 48 h. The intracellular TG content was finally examined using a commercial assay kit at a wavelength of 492 nm after cells were washed with PBS. Protein concentrations were determined using a BCA protein assay kit at a wavelength of 562 nm. TG concentrations were normalized to the total protein content.

Western blot analysis. Protein isolation and western blotting were performed as described previously (29). Cells were homogenized in ice-cold RIPA lysis buffer for 30 min on ice to yield protein samples. The insoluble protein solution was removed by centrifugation at 10,000 x g, 4˚C for 10 min. The supernatant was collected from the lysates, and protein concentrations were determined using the BCA protein assay kit following the manufacturer's instructions. Equal amounts of proteins (40 μg) were resolved by SDS-PAGE on 8% gels and transferred onto PVDF membranes. The membranes were blocked with 5% non-fat dry milk in TBST buffer for 1.5 h at room temperature. The membranes were incubated overnight at 4˚C with primary antibodies (1:500). The blots were rinsed five times with TBST buffer for 6 min each. The washed blots were incubated with a HRP-conjugated secondary antibody (1:5,000) for 1 h at room temperature, then washed five times with TBST buffer. The

Table I. Top list of hit compounds (score value >50 kcal/mol).

Compound no.	Compound name	Score[b], kcal/mol	PubChem CID/CAS no.[c]
Reference[a]	991	64.08	45256693
152	Acotarin D	64.2332	2306174-08-1
803	(E,E)-terrestribisamide	63.872	5321825
804	N-p-coumaroyl-N'-feruloylputrescine	60.2194	44241259
656	6'-benzoate phloroglucinol 1-β-D-glucopyranoside	59.2064	2407648-32-0
1211	Demethoxycurcumin	58.5833	5469424
1145	Liquiritin	57.6091	503737
1209	5-hydroxy-7-(4-hydroxy-3-methoxyphenyl)-1-phenyl-3-heptanone	57.2732	5318228
545	Ononin	56.276	442813
162	7S,8R-erythro-4,7,9,9'-tetrahydroxy-3,3'-dimethoxy-8-O-4'-neolignan	56.1007	13893597
1148	Licochalcone-A	55.7685	5318998
374	Epimedokoreanin D	55.6196	5315125
161	3-[2-(3,4-dimethoxyphenyl)-3-(hydroxymethyl)-7-methoxy-2,3-dihydrobenzofuran-5-yl]-1-propanol	55.1088	4639677
283	(-)-secoisolariciresinol	55.0016	11552274
578	(7S,8R)-3,3',5-trimethoxy-4',7-epoxy-8,5'-neolignan-4,9,9'-triol	54.7096	56838440
522	(-)-Catechin	54.2336	73160
540	Malaferin C	54.1877	71596193
1073	Rosmarinic acid	54.0327	5281792
375	2-(3,4-dihydroxy-5-(3-methylbut-2-enyl)phenyl)-5,7-dihydroxy-8-(2-hydroxy-3-methylbut-3-enyl)chromen-4-one	53.9136	131676094
567	2-(4-hydroxy-3,5-dimethoxyphenyl)ethyl-β-D-glucopyranoside	53.9011	76308955
615	Methyl 5-O-caffeoylquinic acid methyl ester	53.8888	6476139
441	5,7-dihydroxy-3',4',6-trimethoxyflavone	53.8865	5273755
1214	Arctigenin	53.7069	64981
1011	p-hydroxybenzoyl-β-D-glucopyranoside	53.6545	14132342
1195	Curcumin	53.6135	969516
395	3'-(2-hydroxy-3-methyl-3-butenyl)-4',3,5,7-tetrahydroxy-5'-prenylflavone	53.1348	1812887-75-4
1007	3,4-dimethoxycinnamyl-β-D-glucopyranoside	52.7184	21581586
287	4-O-caffeoylquinic acid methyl ester	52.6425	71720840
396	3'-Prenylnaringenin	52.5223	5315396
1012	4-methoxybenzyl-β-D-glucopyranoside	52.4808	10685601
566	3-methoxyphenethyl-alcohol-4-O-β-D-glucopyranoside	52.2909	23815379
284	(-)-arctigenin	52.1262	119205
867	Salidreoside	52.0402	159278
1147	Glabridin	52.023	124052
376	2-(3,4-dihydroxy-5-(3-methylbut-2-en-1-yl)phenyl)-5-hydroxy-8-(2-hydroxypropan-2-yl)-8,9-dihydro-4H-furo(2,3-h)chromen-4-one	51.9827	2196202-19-2
553	(-)-Epicatechin	51.8918	72276
143	Leonurine	51.8901	161464
1196	Desmethoxy curcumin	51.6991	5469424
982	(2R,3R)-3,5,6,7,4'-Pentahydroxyflavanonol	51.6525	101353295
160	Dihydrodehydrodiconiferyl alcohol	51.4808	4365980
1205	(R)-5-hydroxy-1,7-diphenyl-3-heptanone	51.4631	46213118
1140	Hesperidin	51.3406	72281
137	Phenethyl-β-D-glucopyranoside	51.1543	11289099
669	5,6,7,3',4'-pentamethoxyflavone	51.1409	145659
560	Isotachioside	51.1143	15098566
166	N-trans ferulic acid casein amide	51.0104	5280537
19	Luteolin	51.0005	5280445

Table I. Continued.

Compound no.	Compound name	Score[b], kcal/mol	PubChem CID/CAS no.[c]
19	Luteolin	51.0005	5280445
752	2-methyl-3-O-β-D-glucopyranosyl-pyran-4-one	50.6335	5316639
1197	7-(4'-hydroxy-3'-methoxyphenyl)-1-phenyl-4E-heptene-3-one	50.5732	5318278
371	3,6,7-trimethoxy-9,10-dihydrophenanthrene-2,5-diol	50.5535	14135385
552	(+)-Taxifolin	50.2719	439533
900	3-O-trans-coumaroylquinic acid	50.2104	11078262
665	2S-eriodictyol	50.1198	440735
434	Artemetin	50.0462	5320351
382	4,5-Phenanthrenediol, 9,10-dihydro-2,3,6-trimethoxy-9,10-Dihydrophenanthrene	50.0364	25141334

[a]Reference ligand in 4CFE; [b]CDOCKER interaction energy, [c]For compounds without a PubChem CID, the CAS no. is provided.

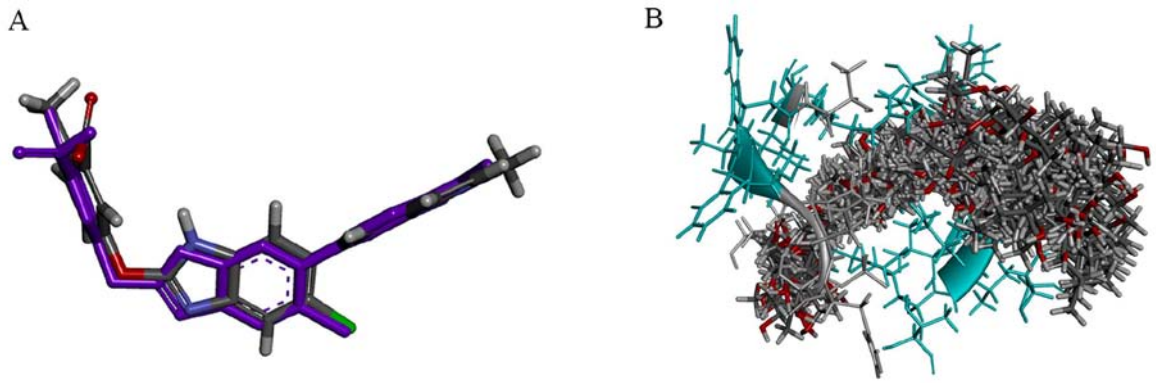

Figure 3. Docking results of 4CFE. (A) Comparison of initial conformation (purple) and virtual docking conformation (gray) of ligand 991 (reference ligand). (B) Overlap of hit compounds.

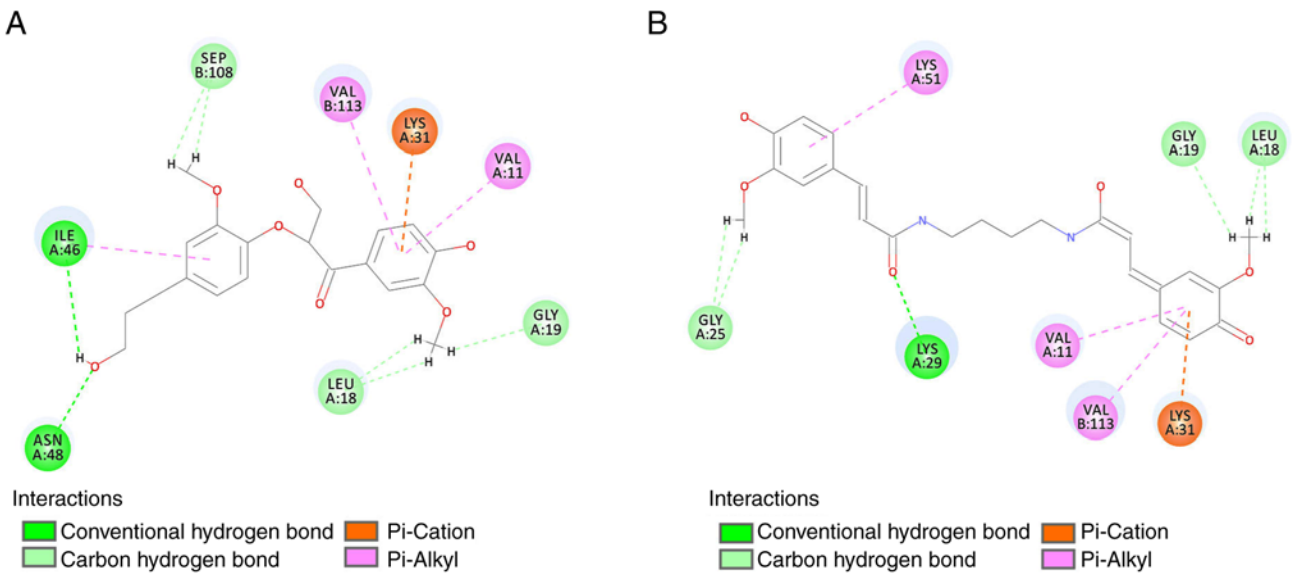

Figure 4. 2D interaction diagram of the top two hits. (A) Acotarin D (compound 152). and (B) (E,E)-terrestribisamide (compound 803).

protein bands were visualized with an enhanced chemiluminescence detection kit (EMD Millipore). The optical density of each band was quantified using ImageJ software v1.53c (National Institutes of Health) and expressed as arbitrary units.

Table II. Selected compounds list for activity verification.

Compound no.	Compound name
1145	Liquiritin
545	Ononin
441	5,7-dihydroxy-3',4',6-trimethoxyflavone
143	Leonurine
522	(-)-Catechin
19	Luteolin
1148	Licochalcone A

Statistical analysis. Statistical analysis was performed using one-way ANOVA followed by Tukey's post hoc test for multiple comparisons. All data are expressed as the mean ± SEM, n=5. $P<0.05$ was considered to indicate a statistically significant difference.

Results and Discussion

Pharmacophore model generation and validation. A total of ten pharmacophore models were generated based on the spatial arrangement of key chemical features from the training set (details in supporting information Table SII). Each of these models contained at least three features.

The top ranked model (HipHop1) was chosen as the best hypothesis containing one hydrophobic region feature and two hydrogen bond acceptor lipid (Ali1 and Ali2) features (Fig. 1A). The hydrophobic region feature was farther from the other two hydrogen bond acceptor lipid features. The pharmacophore hypotheses matched well with those potent ligands, especially with initial ligand 991. The pharmacophore model was also validated using the Ligand profiler method from the Discovery Studio software.

Virtual screening based on pharmacophore. The natural product library, consisting of 1,235 natural compounds, was constructed using Build 3D database modular. The screening based on pharmacophore was conducted using the Search 3D database. All the hit compounds were aligned in the pharmacophore model in Fig. 2. Compared with the binding site structure, the distance between the hydrophobic region feature and the other two hydrogen bond acceptor lipid features facilitated hydrogen bond interactions between ligands and amino acid residues B:ASN111, A:LYS29, B:THR106, and B:phosphoserine (SER)108 in the AMPK activation site and was also beneficial for hydrophobic interactions between ligands and the hydrophobic region of the receptor.

Molecular docking. Benzimidazole derivative 991 is a well-characterized direct AMPK activator binding in the specific binding site of AMPK. The 3D crystal structure of AMPK-ligand (991) complex draws a distinct image of this specific binding site, and paves a convenient way for screening of direct AMPK activators (30,31). To verify the applicability of the binding site model for AMPK docking screening, a redocking process was utilized, starting from a random conformation of the initial ligand 991. The RMSD value between the initial conformation and virtual docking conformation was 1.4035 Å (Fig. 3A). This result illustrated that this binding site model could simulate the real ligand binding model (real crystal structure of Benzimidazole derivative 991 binding to the active site of AMPK) and could be appropriate for further docking studies.

The hit compounds from the pharmacophore screening were subjected to the CDOCKER docking process, resulting in 284 hit compounds for *in vitro* activity studies. The hit compounds were aligned in Fig. 3B, and all hit compounds from the docking study displayed similar spatial conformations. The top 54 hit compounds (score >50 kcal/mol) are listed in Table I (details of these compounds Table SIII and Fig. S2).

The 2D interaction diagram of the top two hits, acotarin D and (E,E)-terrestribisamide, indicates that the residues A:Gly19, A:Leu18, A:ILE46, A:ASN48, B:SEP108, A:Gly25, and A:Lys29 were involved in the formation of hydrogen bonds; the residues A:Lys31, B:VAL113 and A:VAL11 were involved in the formation of hydrophobic interactions (Fig. 4).

TG accumulation inhibitory effects of selected compounds. AMPK is a key sensor that maintains the balance of energy metabolism by regulating glucose and lipid metabolism. Activation of AMPK leads to increases in fatty acid oxidation though multiple pathways such as activation of malonyl CoA decarboxylase and reduction of the inhibitory effect of malonyl CoA to carnitine palmitoyl transterase-1 (1,2). Therefore, inhibition of TG accumulation is a preliminary indicator for AMPK activation (29).

TG accumulation inhibitory assays were carried out for preliminary activity screening in sodium oleate-treated HepG2 cells. Considering docking score and structural diversity, seven compounds (Table II) with a score >50 kcal/mol were selected and evaluated for their inhibitory effects on TG accumulation.

Following sodium oleate challenge, the intracellular TG levels increased almost four-fold in the model group (Fig. 5), compared with the control. However, this increase in TG levels induced by sodium oleate was significantly reduced by ~13.8% following orlistat treatment. Moreover, 30 μM (-)-catechin (compound 522), luteolin (compound 19), and licochalcone A (compound 1148) also significantly reduced intracellular TG levels by 13.4, 9.7 and 7.7%, respectively. In addition, (-)-catechin also exhibited a moderate inhibitory effect on TG accumulation at a concentration of 3 μM. The other compounds did not result in any detectable effects.

AMPK phosphorylation effect of selected compounds in sodium oleate-induced HepG2 cells. The activation effects of (-)-catechin (compound 522), luteolin (compound 19), and licochalcone A (compound 1148) on AMPK were further assessed. Immunoblotting analysis indicated that AMPK phosphorylation levels significantly decreased after 200 μM sodium oleate challenge in the model group (Fig. 6), compared with the control. Among the tested compounds, compound 522 [(-)-catechin] and 1148 (licochalcone A) significantly increased AMPK phosphorylation levels at a concentration of 30 μM, as evidenced by higher p-AMPK/t-AMPK ratios. However, other selected compounds had no apparent effect on AMPK phosphorylation.

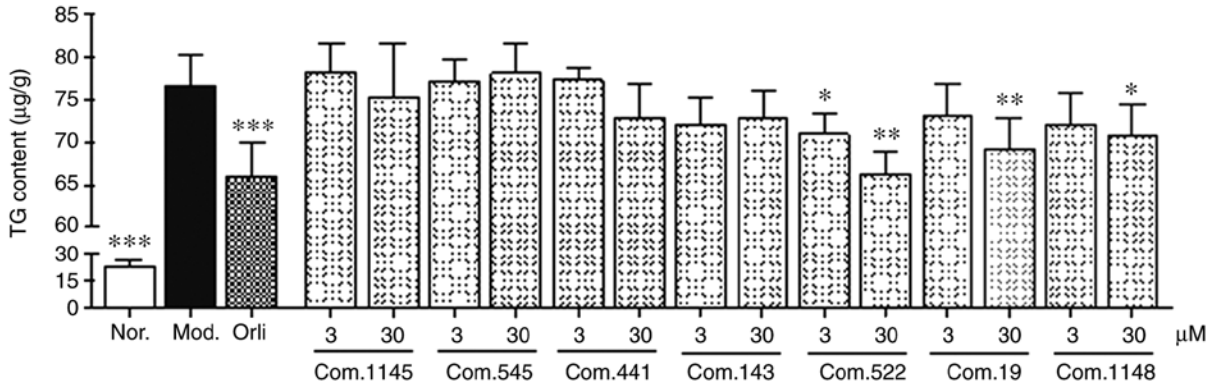

Figure 5. TG accumulation inhibitory assay. Data are presented as the mean ± SEM. n=5. ***P<0.001, **P<0.01, *P<0.05 vs. model group. TG, triglyceride, Com.; compound; Mod., model; Nor., normal; Orli., orlistat treatment.

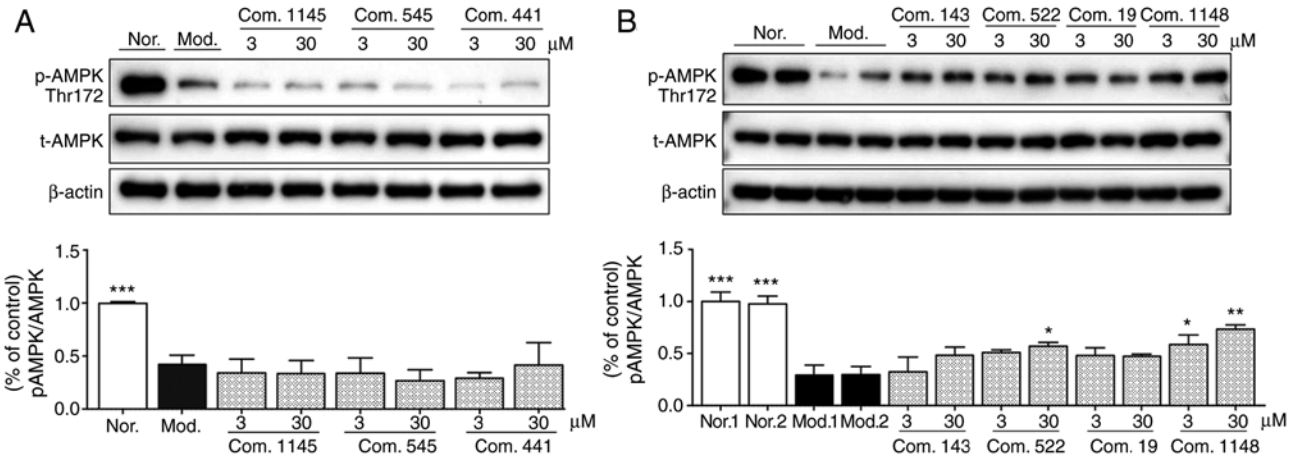

Figure 6. AMPK activation assay. Data are presented as the mean ± SEM. (A) Results for com. 1145, com. 545, and com. 441. ***P<0.001 vs. Mod. (B) Results for com. 143, com. 522, com. 19, and com. 1148. ***P<0.001, **P<0.01, *P<0.05 vs. Mod. 1. AMPK, adenosine monophosphate-activated protein kinase; Com., compound; Mod., model; Nor., normal; p, phosphorylated; t, total.

Comparing the results of the TG accumulation and the AMPK phosphorylation assays, the activity trends of these two tests were consistent, and compound 522 [(-)-catechin] and 1148 (licochalcone A) performed well in both assays. Our findings agreed with the results of previous studies indicating that both compounds 522 [(-)-catechin] and 1148 (licochalcone A) are potential AMPK activators (32,33). According to the docking results, these two natural products may directly modulate AMPK activity in an AMP-independent way by binding to the specific binding site.

Conclusions. The present study followed on our research efforts on the separation and purification of natural compounds from traditional Chinese herbs. In this study, virtual screening for direct natural AMPK activators was conducted using a combination of ligand- and structure-based screening. The hit compounds displayed similar spatial conformations and bound to the AMPK-specific binding site through hydrogen bonds and hydrophobic interactions. A total of seven hit compounds were chosen for subsequent activity validation. (-)-Catechin (compound 522) and licochalcone A (compound 1148) performed well in two activity tests and could be valuable for further pharmacological evaluation. The present findings suggest that these two natural products may directly modulate AMPK activity in an AMP-independent manner, through the specific binding site of AMPK. This study may provide insight into the development of AMPK activators from natural resources and their modulatory mechanisms.

Acknowledgements

Not applicable.

Funding

This project was supported by the National Natural Science Foundation (grant nos. 81673703 and 81803691), and the Important Drug Development Fund, Ministry of Science and Technology of China (grant nos. 2018ZX09735-002 and 2019ZX09201005-002-007).

Availability of data and materials

The datasets generated and/or analyzed during the current study are available from the corresponding author on reasonable request.

Authors' contributions

TW designed the experiment and was responsible for the conception of the study. JH, ZY and LH performed the laboratory experiments and wrote the manuscript. JL and YZ contributed to the pharmacological experiments. All authors read and approved the final manuscript.

Ethics approval and consent to participate

Not applicable.

Patient consent for publication

Not applicable.

Competing interests

The authors declare that they have no competing interests.

References

1. Gruzman A, Babai G and Sasson S: Adenosine monophosphate-activated protein kinase (AMPK) as a new target for antidiabetic drugs: A review on metabolic, pharmacological and chemical considerations. Rev Diabet Stud 6: 13-36, 2009.
2. Daskalopoulos EP, Dufeys C, Bertrand L, Beauloye C and Horman S: AMPK in cardiac fibrosis and repair: Actions beyond metabolic regulation. J Mol Cell Cardiol 91: 188-200, 2016.
3. Shirwany NA and Zou MH: AMPK: A cellular metabolic and redox sensor. A minireview. Front Biosci (Landmark Ed) 19: 447-474, 2014.
4. Gejjalagere Honnappa C and Mazhuvancherry Kesavan U: A concise review on advances in development of small molecule anti-inflammatory therapeutics emphasising AMPK: An emerging target. Int J Immunopathol Pharmacol 29: 562-571, 2016.
5. Kim J, Yang G, Kim Y, Kim J and Ha J: AMPK activators: Mechanisms of action and physiological activities. Exp Mol Med 48: e224, 2016.
6. Plews RL, Mohd Yusof A, Wang C, Saji M, Zhang X, Chen CS, Ringel MD and Phay JE: A novel dual AMPK activator/mTOR inhibitor inhibits thyroid cancer cell growth. J Clin Endocrinol Metab 100: E748-E756, 2015.
7. Law BY, Mok SW, Chan WK, Xu SW, Wu AG, Yao XJ, Wang JR, Liu L and Wong VK: Hernandezine, a novel AMPK activator induces autophagic cell death in drug-resistant cancers. Oncotarget 7: 8090-8104, 2016.
8. Grahame Hardie D: Regulation of AMP-activated protein kinase by natural and synthetic activators. Acta Pharm Sin B 6: 1-19, 2016.
9. Polekhina G, Gupta A, Michell BJ, van Denderen B, Murthy S, Feil SC, Jennings IG, Campbell DJ, Witters LA, Parker MW, *et al*: AMPK beta subunit targets metabolic stress sensing to glycogen. Curr Biol 13: 867-871, 2003.
10. Lefort N, St-Amand E, Morasse S, Côté CH and Marette A: The alpha-subunit of AMPK is essential for submaximal contraction-mediated glucose transport in skeletal muscle in vitro. Am J Physiol Endocrinol Metab 295: E1447-E1454, 2008.
11. Day P, Sharff A, Parra L, Cleasby A, Williams M, Hörer S, Nar H, Redemann N, Tickle I and Yon J: Structure of a CBS-domain pair from the regulatory gamma1 subunit of human AMPK in complex with AMP and ZMP. Acta Crystallogr D Biol Crystallogr 63(Pt 5): 587-596, 2007.
12. Hardie DG, Ross FA and Hawley SA: AMPK: A nutrient and energy sensor that maintains energy homeostasis. Nat Rev Mol Cell Biol 13: 251-262, 2012.
13. Gowans GJ, Hawley SA, Ross FA and Hardie DG: AMP is a true physiological regulator of AMP-activated protein kinase by both allosteric activation and enhancing net phosphorylation. Cell Metab 18: 556-566, 2013.
14. Xiao B, Sanders MJ, Carmena D, Bright NJ, Haire LF, Underwood E, Patel BR, Heath RB, Walker PA, Hallen S, *et al*: Structural basis of AMPK regulation by small molecule activators. Nat Commun 4: 3017, 2013.
15. Zadra G, Photopoulos C, Tyekucheva S, Heidari P, Weng QP, Fedele G, Liu H, Scaglia N, Priolo C, Sicinska E, *et al*: A novel direct activator of AMPK inhibits prostate cancer growth by blocking lipogenesis. EMBO Mol Med 6: 519-538, 2014.
16. Newman DJ and Cragg GM: Natural products as sources of new drugs over the nearly four decades from 01/1981 to 09/2019. J Nat Prod 83: 770-803, 2020.
17. Wang T, Ruan J, Li X, Chao L, Shi P, Han L, Zhang Y and Wang T: Bioactive cyclolanstane-type saponins from the stems of Astragalus membranaceus (Fisch.) Bge. var. mongholicus (Bge.) Hsiao. J Nat Med 70: 198-206, 2016.
18. Zhang Y, Chao L, Ruan J, Zheng C, Yu H, Qu L, Han L and Wang T: Bioactive constituents from the rhizomes of Dioscorea septemloba, Thunb. Fitoterapia 115: 165-172, 2016.
19. Zhang Y, Nakamura S, Nakashima S, Wang T, Yoshikawa M and Matsuda H: Chemical structures of constituents from the seeds of Cassia auriculata. Tetrahedron 71: 6727-6732, 2015.
20. Zhang Y, Han L, Ge D, Liu X, Liu E, Wu C, Gao X and Wang T: Isolation, structural elucidation, MS profiling, and evaluation of triglyceride accumulation inhibitory effects of benzophenone C-glucosides from, leaves of mangifera indica L. J Agric Food Chem 61: 1884-1895, 2013.
21. Lee YK, Lee WS, Hwang JT, Kwon DY, Surh YJ and Park OJ: Curcumin exerts antidifferentiation effect through AMPKalpha-PPAR-gamma in 3T3-L1 adipocytes and antiproliferatory effect through AMPKalpha-COX-2 in cancer cells. J Agric Food Chem 57: 305-310, 2009.
22. Liu Z, Cui C, Xu P, Dang R, Cai H, Liao D, Yang M, Feng Q, Yan X and Jiang P: Curcumin activates AMPK pathway and regulates lipid metabolism in rats following prolonged clozapine exposure. Front Neurosci 11: 558, 2017.
23. Price NL, Gomes AP, Ling AJ, Duarte FV, Martin-Montalvo A, North BJ, Agarwal B, Ye L, Ramadori G, Teodoro JS, *et al*: SIRT1 is required for AMPK activation and the beneficial effects of resveratrol on mitochondrial function. Cell Metab 15: 675-690, 2012.
24. Jin Y, Liu S, Ma Q, Xiao D and Chen L: Berberine enhances the AMPK activation and autophagy and mitigates high glucose-induced apoptosis of mouse podocytes. Eur J Pharmacol 794: 106-114, 2017.
25. Kim SG, Kim JR and Choi HC: Quercetin-induced AMP-activated protein kinase activation attenuates vasoconstriction through LKB1-AMPK signaling pathway. J Med Food 21: 146-153, 2018.
26. Han YH, Kee JY, Park J, Kim HL, Jeong MY, Kim DS, Jeon YD, Jung Y, Youn DH, Kang J, *et al*: Arctigenin inhibits adipogenesis by inducing AMPK activation and reduces weight gain in high-fat diet-induced obese mice. J Cell Biochem 117: 2067-2077, 2016.
27. Wu G, Robertson DH, Brooks CL III and Vieth M: Detailed analysis of grid-based molecular docking: A case study of CDOCKER-A CHARMm-based MD docking algorithm. J Comput Chem 24: 1549-1562, 2003.
28. Patel Y, Gillet VJ, Bravi G and Leach AR: A comparison of the pharmacophore identification programs: Catalyst, DISCO and GASP. J Comput Aided Mol Des 16: 653-681, 2002.
29. Zhang Y, Liu X, Han L, Gao X, Liu E and Wang T: Regulation of lipid and glucose homeostasis by mango tree leaf extract is mediated by AMPK and PI3K/AKT signaling pathways. Food Chem 141: 2896-2905, 2013.
30. Potunuru UR, Priya KV, Varsha MKNS, Mehta N, Chandel S, Manoj N, Raman T, Ramar M, Gromiha MM and Dixit M: Amarogentin, a secoiridoid glycoside, activates AMP-activated protein kinase (AMPK) to exert beneficial vasculo-metabolic effects. Biochim Biophys Acta Gen Subj 1863: 1270-1282, 2019.
31. Mok SWF, Zeng W, Niu Y, Coghi P, Wu Y, Sin WM, Ng SI, Gordillo-Martínez F, Gao JY, Law BYK, *et al*: A method for rapid screening of anilide-containing AMPK modulators based on computational docking and biological validation. Front Pharmacol 9: 710, 2018.
32. Hwang JT, Park OJ, Lee YK, Sung MJ, Hur HJ, Kim MS, Ha JH and Kwon DY: Anti-tumor effect of luteolin is accompanied by AMP-activated protein kinase and nuclear factor-KB modulation in HepG2 hepatocarcinoma cells. Int J Mol Med 28: 25-31, 2011.
33. Bae UJ, Park J, Park IW, Chae BM, Oh MR, Jung SJ, Ryu GS, Chae SW and Park BH: Epigallocatechin-3-Gallate-rich green tea extract ameliorates fatty liver and weight gain in mice fed a high fat diet by activating the sirtuin 1 and AMP activating protein kinase pathway. Am J Chin Med 46: 617-632, 2018.